



Contents lists available at ScienceDirect

Colloids and Surfaces B: Biointerfaces

journal homepage: www.elsevier.com/locate/colsurfb

Controlling fibrinogen adsorption on polyelectrolyte multilayer films by modifying self-assembly conditions

Borislava Borisova^a, Sonia Apostolova^a, Irina Georgieva^a, Marina Ivanova^a, Rumen Krastev^b, Rumiana Tzoneva^{a,*}, Tonya Andreeva^{a,b,**}

^a Institute of Biophysics and Biomedical Engineering, Bulgarian Academy of Sciences, Acad. G. Bonchev Str., Bl. 21, Sofia 1113, Bulgaria

^b Faculty Life Sciences, Reutlingen University, Alteburgstraße 150, Reutlingen 72762, Germany

ARTICLE INFO

Keywords:

Polyelectrolyte multilayers (PEM)
Surface properties
Wettability
Surface charge
Coatings
Fibrinogen adsorption

ABSTRACT

This study investigates the relationship between fibrinogen adsorption on polyelectrolyte multilayer (PEM) films and their surface properties. The films were constructed using weak polyelectrolytes, poly(acrylic acid) (PAA), and poly(allylamine hydrochloride) (PAH), with polyethyleneimine (PEI) as a precursor layer. Different deposition conditions, such as pH levels (3.5 and 7.0) and the type of outermost layer (PAA or PAH), were used to create films with tunable hydrophilicity and surface charge. The thickness of these films was measured using ellipsometry, and surface wettability was assessed via the contact angle method. Fibrinogen adsorption was quantified using quartz crystal microbalance with dissipation monitoring (QCM-D) and enzyme immunoassay (EIA) method, focusing on its D-domain exposure concerning surface thrombogenicity. Results indicated that PEM films are generally hydrophilic. Among them, PAH, the outermost layer, is the least hydrophilic and, therefore, has the lowest surface energy. Film thickness varied with the pH of the solutions, creating a mechanism to control layer parameters. Fibrinogen adsorption was more pronounced on less hydrophilic surfaces, which were thinner, viscoelastic, more hydrated, and preferentially positively charged. These findings suggest that by controlling surface properties, one can enhance hemocompatibility by influencing fibrinogen adsorption and subsequent platelet adhesion and activation.

1. Introduction

Polyelectrolyte multilayer (PEMs) thin films, constructed with layer-by-layer (LbL) technology applying alternating layers of two polyelectrolytes, are known for their exceptional stability controlled by the increase of entropy due to the release of small counterions [1,2]. The surface properties of PEMs, including surface chemistry and biocompatibility, can be finely tuned by adjusting parameters such as the choice of polyelectrolytes, the number of assembled layers, and the deposition conditions like pH [1,2]. The stability and versatility of PEMs make them reliable as coatings of implantable biomedical devices [2]. The selection of polyelectrolyte pairs and process parameters during PEM fabrication influences their physicochemical properties and enables precise control over protein adsorption on PEM-coated biomaterials.

The interaction between medical implants and biological tissues is a

key problem of the contemporary biomedical sciences [3]. Thrombus formation on artificial surfaces poses a significant challenge for blood-interacting materials. When a biomaterial contacts blood, the first event is the formation of a layer of adsorbed plasma proteins on the surface, which then mediates biological responses to these biomaterials. In surface-induced thrombosis, FNG plays a prominent role in facilitating thrombosis development by mediating platelet adhesion and aggregation to biomaterials [4,5]. The adsorbed FNG can bind to platelets through cell membrane receptors, including GPIIb/IIIa (integrin α IIb β 3), and GPIb. This binding induces platelet adhesion and aggregation [6]. Therefore, studying protein adsorption processes before applying the biomaterials is essential to developing better hemocompatible devices.

Several studies have suggested that platelet adhesion and activation might be particularly affected by the conformation of FNG upon adsorption [7–11]. The influence of materials surface properties on FNG

* Corresponding author.

** Correspondence to: Reutlingen University, Alteburgstrasse 150, 72762 Reutlingen, Germany.

E-mail addresses: bobi4borissova@gmail.com (B. Borisova), sonia_apostolova@yahoo.com (S. Apostolova), georgieva.irina5@gmail.com (I. Georgieva), mmivanova14@gmail.com (M. Ivanova), Rumen.Krastev@Reutlingen-University.DE (R. Krastev), tzoneva@bio21.bas.bg (R. Tzoneva), Tonya.Andreeva@Reutlingen-University.DE (T. Andreeva).

<https://doi.org/10.1016/j.colsurfb.2025.114821>

Received 20 April 2025; Received in revised form 16 May 2025; Accepted 23 May 2025

Available online 27 May 2025

0927-7765/© 2025 The Author(s). Published by Elsevier B.V. This is an open access article under the CC BY-NC-ND license (<http://creativecommons.org/licenses/by-nc-nd/4.0/>).

adsorption and conformation has been widely studied [12–15], and it was accepted that the conformational changes are surface-dependent [16,17]. Distorted conformations may impede function and expose hidden epitopes that can cause unintended effects on biological functions [18]. Furthermore, adsorption-induced rearrangements and crowding effects may enhance protein-protein interactions and aggregation. The latter issue has been extensively studied, particularly regarding protein misfolding and platelet aggregation [19]. Consequently, molecular-level descriptions of protein adsorption would significantly enhance our understanding of the phenomenon and are crucial for effectively regulating protein-surface interactions [20].

Surface wettability is one of the factors discussed in terms of its effects on FNG adsorption. For instance, researchers observed intensified structural deformation of FNG as the hydrophobicity of the material surface increases [6]. Quantitative analysis of the different domains showed that the overall molecular lengths and widths of the individual D and E domains increased. At the same time, their heights decreased as the material surface became more hydrophobic [17]. The higher affinity and more significant protein adsorption onto more hydrophobic surfaces is probably due to their protein's larger size and its ability to form sufficient contacts after adjusting its orientation. [21,22]. FNG was found to adsorb more rapidly to hydrophilic surfaces and lose an ordered secondary structure over a much longer timescale than to hydrophobic surfaces [17]. Surface free energy, charge, microroughness, and degree of hydroxylation are other crucial surface parameters that affect protein adsorption and cell behavior on biomaterial surfaces [12]. The complex nature of protein adsorption explains why a complete and comprehensive explanation is still missing.

In this study, we investigate the impact of the surface properties of ultra-thin PEM films (PAA/PAH) on the adsorption of human FNG. By altering the pH during film assembly and the outermost layer, we created surfaces with varying hydrophilicity and surface charge, influencing FNG adsorption and its D-domain conformation/orientation upon adsorption. Understanding the dynamics of FNG adsorption and the exposure of its functional domains is essential for comprehending and potentially manipulating the thrombus formation process on the PEM-coated biomaterial surface.

2. Materials and methods

2.1. Layer-by-layer deposition of PEMs

The PEM films were assembled with the layer-by-layer (LbL) dip coating technique consisting of consecutive and repeated deposition of the polyanion poly(acrylic acid), PAA (Sigma Aldrich, Mw ~100 kDa), and the polycation poly(allylamine hydrochloride), PAH (Thermo Scientific, Mw 120–200 kDa), following the protocol described in [23]. Branched poly(ethyleneimine), PEI (Sigma Aldrich, Mw ~750 kDa) was used as a precursor layer to provide better adhesion of the coating to the substrate [24]. The working concentration of the polyelectrolytes was 2 mg/mL. 0.5 M NaCl (Carl Roth GmbH, Germany) was added to the PAA and PAH solutions. Salts affect the electrostatic interactions between the layers, leading to structural integrity and stability changes [25].

The use of PEI as a precursor layer has raised concerns over the years due to its potential cytotoxicity. Studies have demonstrated that PEI can exert adverse effects on cells, with toxicity largely influenced by factors such as molecular weight, concentration, exposure duration, and cell type involved [26,27]. These studies, however, primarily involved the direct application of PEI as a single or terminating layer in direct contact with cells. In contrast, our study utilizes PEI solely as an initial anchoring layer to facilitate the controlled and uniform deposition of PEMs, a widely established strategy in surface modification and biomaterials engineering [28,29]. Importantly, the PEI layer is immediately covered by several bilayers of oppositely charged polyelectrolytes, effectively isolating it from direct contact with cells and biological fluids. Previous research has shown that the addition of even a few

polyelectrolyte bilayers is sufficient to neutralize the cytotoxicity of PEI by shielding its interaction with the biological environment [30]. In our own extensive *in vitro* studies, we have demonstrated that PEM coatings anchored with PEI do not exhibit cytotoxic effects on a variety of cell types, including fibroblasts, osteoblasts, and human umbilical vein endothelial cells (HUVECs) [31]. Moreover, we observed enhanced cytocompatibility on otherwise cytotoxic substrates—such as magnesium-based stents—following PEM functionalization anchored with PEI, further supporting the biocompatibility of this approach [31].

A total of four PEM films were assembled. (PAA/PAH)₅ films (with PAH as the outermost layer) and (PAA/PAH)_{5,5} films (with PAA as the outermost layer) were assembled from PAA and PAH solutions with pH of either 3.5 or 7.0. The films are labeled PAA 7.0, PAH 7.0, PAA 3.5, and PAH 3.5, with the abbreviations indicating the pH of the polyelectrolyte solutions and the identity of the outermost layer. The PEM films were applied to different substrates by the requirements of the methods used for subsequent testing and characterization - sterile polystyrene 96 well plates (Corning Inc., New York, USA) for indirect enzyme immunoassay (EIA), glass slides for the contact angle measurements, silicon (100) (Si)-wafers (10 × 10 mm, CrysTec GmbH, Berlin, Germany) for the ellipsometry and quartz crystal gold (Au) chips (3 T Analytik, Germany) for the Quartz crystal measurement with dissipation monitoring (QCM-D). The cleaning procedure for the substrates involved two or three sequential steps performed in an ultrasonic bath at room temperature. Glass slides were cleaned in Mucosol® (Schülke & Mayr GmbH, Germany), acetone, and isopropanol, with each step lasting 2 minutes. Si-wafers underwent cleaning in acetone and isopropanol. The use of different substrate materials in this study necessitated the application of PEM coatings consisting of 5.5 or 6.0 bilayers (including the initial PEI anchoring layer). This choice was based on previous studies indicating that complete and uniform surface coverage is typically achieved after 4–6 deposition cycles [32,33]. Beyond this threshold, the influence of the substrate's surface chemistry and charge diminishes significantly, and the subsequent multilayer buildup becomes governed primarily by the properties of the polyelectrolytes themselves rather than the underlying material. This ensures consistent film thickness, morphology, and physicochemical properties across all substrates, thereby enabling reliable comparison of surface-dependent biological interactions.

2.2. Static water contact angle and surface free energy

A contact angle goniometer (Dataphysics GmbH, Filderstadt, Germany) was utilized to quantify the static water contact angles (CA) of multilayer films, as described in [34]. The sessile drop method was employed by dispensing 4 µL of deionized ultrapure water onto the surface. The droplet's shape was analyzed using the Young-Laplace equation. Measurements were taken at three random locations on each of three samples per condition, resulting in a total of nine measurements to determine the average contact angle and standard deviation.

The surface free energy (SFE) of each PEM was analyzed by measuring the static contact angles with deionized ultrapure water (Sartorius, Germany, purity of 0.055 µS/cm c at 20.0 °C), glycerin (99.5 %, Carl Roth, Germany), and n-hexadecane (99 %, Carl Roth, Germany). The Owens, Wendt, Rabel and Kaelble approach was used to determine the SFE [35]. This method assumes that the SFE (γ) comprises a dispersive component (γ_d) and a polar component (γ_p). The surface tension values of the test liquids at 20 °C were obtained from published data (Table 1).

2.3. Ellipsometry

PEM films' thickness and refractive index were determined using a high-performance spectroscopic ellipsometer Sentech SE800 (Sentech Instruments GmbH, Berlin, Germany). It operates within the spectral range of 280 nm to 850 nm and utilizes an angle of incidence of 70 degrees. A four-layer model was employed to evaluate the optical

Table 1

Surface tension (SFT) with its polar and dispersive parts for deionized water, glycerol, and n-hexadecane.

liquids	surface tension (SFT)		
	SFT total (mN/m)	polar part (mN/m)	dispersive part (mN/m)
deionized water, Ström et. al (33)	72.8	51.0	21.8
glycerol, Ström et. al (33)	63.4	26.4	37.0
n-hexadecane, Jasper et. al (34)	27.5	0	27.5

properties of thin films layered on the substrates. This model considers the following layers: ambient medium (air, water, or phosphate buffered saline (PBS), pH 7.4), the PEM film whose properties are measured, and the substrate on which the thin film was deposited (consisting of bulk silicon and a silicon dioxide surface layer). A Sentech se800 liquid cell was used to determine the hydrated thickness as described previously. The samples were analyzed in three different spots, and each sample was prepared in triplicate.

2.4. Adsorption of Methylene blue and Alizarin red

The surface charges of PEMs were characterized by quantifying electrostatic interactions between the PEM-coated surfaces and charged dye molecules. Methylene blue (MB), a monocationic dye, has been previously utilized to determine the number of surface anionic charges [36]. In this study, we introduce alizarin red (AR), a monoanionic dye, as a novel method for estimating the number of surface cationic charges. The PEM-coated substrates were incubated in 1 mM MB solution or 1 mM AR solution for 6 minutes, followed by five washing steps, each lasting 1 minute. The number of adsorbed MB and AR molecules was determined by absorbance measurements using a Lambda Bio+ UV-Vis Spectrometer (PerkinElmer, MA, USA). MB absorbance was measured at 660 nm, while AR absorbance was measured at 260 nm. The quantities of surface-exposed positive and negative charges were determined, and from these, the total net surface charge was calculated.

2.5. Quartz crystal microbalance with dissipation monitoring (QCM-D)

The formation of multilayers, along with the quantity and kinetics of FNG adsorption, was monitored *in situ* by QCM-D (qCell T, 3T Analytik, Tuttlingen, Germany). This method provides detailed information on the adsorbed mass, encompassing the films' viscoelastic characteristics. PEM assembly on the Au quartz crystal was carried out following the same LbL protocol described above. Following film construction, the system was equilibrated in PBS. Subsequently, a 1-hour FNG adsorption step was performed using a 0.5 mg/mL FNG solution in PBS, followed by three 2-minute rinses with PBS. The mass of adsorbed FNG was calculated by measuring the frequency change of the QCM and applying the Sauerbrey equation [37] for rigid films, where ΔD is below 5 % of the scaled frequency change [38] (in this study, films built at pH 3.5), and Kanazawa [39] equations for the films built at pH 7.0 with viscoelastic properties. Kanazawa's [39] equations consider liquid properties (density and dynamic viscosity) and layer characteristics (density, thickness, and complex shear modulus) as detailed in [40].

2.6. Indirect enzyme immunoassay (EIA)

As previously described, FNG adsorption on various surfaces was examined using a modified enzyme immunoassay [9]. Unmodified and PEM-modified surfaces were incubated for 1 hour at 37 °C with either 100 % fresh human citrate plasma from healthy volunteers (University Hospital for Neurology and Psychiatry "Sveti Naum", Sofia) or a 10 µg/mL FNG (Sigma Aldrich, Germany, Product No.: F4883) solution

dissolved in PBS. The monoclonal mouse anti-human FNG antibody (Clone 85D4 Sigma, F 9902), which recognizes a conformational sensitive epitope of the gamma chain (302–303), was employed to identify the accessibility of the D-domain, a potential ligand for platelet binding. The assay included a blocking step with 1 % BSA before the primary antibody and washing steps with PBS. After incubating with peroxidase-conjugated anti-mouse IgG (whole molecule) (1:40 000, A9044, Sigma Aldrich, Germany) for 30 minutes, the reaction was developed using 3,3',5,5'-Tetramethylbenzidine tablets (T3405, Sigma Aldrich, Germany) in 0.05 M phosphate citrate buffer (pH 5.01) with 0.03 % hydrogen peroxide for 10 minutes. The reaction was stopped by adding 200 µL of 1 M H₂SO₄, and the optical density (OD) was measured at 450 nm using a plate reader Infinite F200 PRO (Tecan Trading GmbH, Männedorf, Switzerland). Each experiment was conducted at least three times in triplicate.

2.7. Statistical analysis

Data analysis was performed using Graph Pad Prism 5 and Microsoft Excel. Statistical significance was assessed using ANOVA with Tukey's post-hoc test. Results are presented as mean ± standard deviation (St. Dev.), with $p < 0.05$ considered statistically significant. Significance levels are denoted as * $p < 0.05$, ** $p < 0.01$, and *** $p < 0.001$.

3. Results and discussion

3.1. Building and physicochemical characterization of PEM coatings

The real-time monitoring of the growth and viscoelastic properties of PAA/PAH multilayers during their LbL assembly was investigated by analyzing frequency (Δf) and damping (ΔD) changes of the QCM-D crystals. Analysis of the changes in resonance frequency and damping was assessed to account for the viscoelasticity of these films.

The data revealed that at pH 3.5, there is a steep exponential increase in $-\Delta f$ with each deposited layer, indicating progressive and substantial film growth. This suggests that the multilayers formed at low pH are thicker and incorporate more material (and likely water) (Fig. 1). At pH 7.0, the frequency shifts are much slower and less pronounced, implying thinner layers or reduced material deposition per cycle. The minor damping shifts at pH 3.5 are smaller compared to those at pH 7.0, indicating that the films assembled at low pH are more rigid and contain a more significant amount of adsorbed polyelectrolyte mass compared to the films assembled at pH 7.0. Our data are in line with previous studies demonstrating that changing pH during self-assembly of these two weak polyelectrolytes affects the growth regime which is linear at pH close to 7.0 and exponential at lower and higher pH [41]. The switch of the growth regime is attributed to the pH-dependent change in charge density and conformation of the weak PAH and PAA polyelectrolytes [42]. At pH 3.5, PAA exhibits reduced ionization, while PAH is fully charged. The charge mismatch results in a structure with more loops and tails that can accumulate thicker layers. In contrast, at pH 7.0, both PAA and PAH are fully charged, leading to thinner and more interpenetrated layers with flat chains within the multilayer structure. Our findings agree with Shiratori and Rubner [42], who demonstrated that the degree of interpenetration of the multilayers is less at pH 3.5 than at pH 7.0. The data were collected by contact angle measurements and methylene blue staining, indicating some free binding sites and incomplete interpenetration due to the partially charged state of PAA [42]. All four PAA/PAH multilayers studied here were strongly hydrophilic, with contact angles ranging from 11° to 33° (Fig. 2A, Fig. 3A). The assembly pH and outermost layer composition influenced the PEMs' wettability, with PAA-terminated films being more hydrophilic than PAH-terminated ones, consistent with previous studies [42]. The film assembled at pH 7.0 with PAH as the outermost layer was the least hydrophilic, while the film constructed at pH 3.5 with PAA as the final layer was the most hydrophilic. The most pronounced hydrophilicity of the PAA 3.5 film

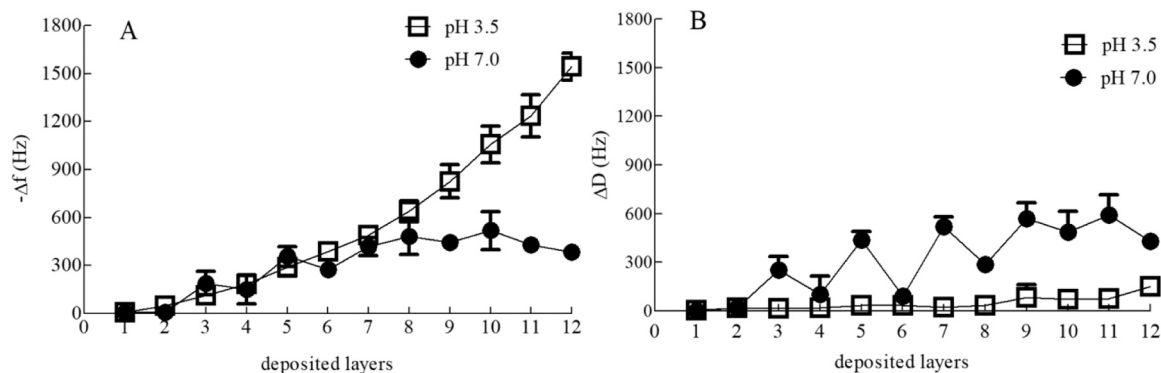


Fig. 1. (A) Frequency change, Δf , and (B) damping change, ΔD , during the LbL deposition of PAA/PAH films at pH 3.5 (squares) and pH 7.0 (circles). Even numbers correspond to PAA deposition, while odd numbers correspond to PAH deposition. Each point was measured in triplicate.

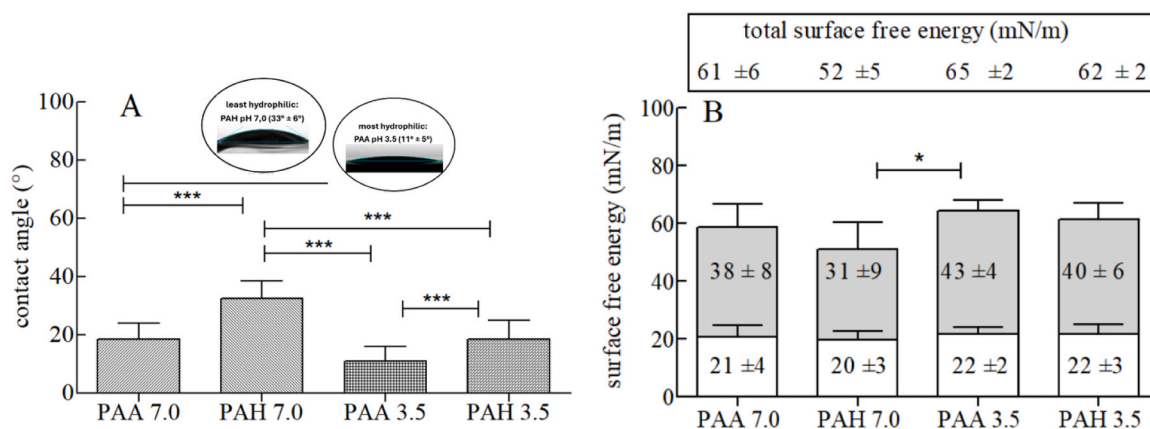


Fig. 2. (A) Static water contact angle and (B) surface free energy of four different PEMs. The bar chart in (B) is segmented into two parts for each sample: the dispersive (white) component and the polar (grey) component of surface free energy. Data are presented as mean \pm St.Dev. Statistical significance: ns - non-significant ($P > 0.05$), * $P \leq 0.05$, ** $P \leq 0.01$, *** $P \leq 0.001$. Three independent experiments were conducted, and each sample was measured in triplicate.

can be attributed to the carboxylic groups in PAA, which readily form hydrogen bonds with water [43]. The number of these groups on the surface increases as the pH of the PAA solution decreases [42].

The surface free energies of the PAA/PAH films constructed under varying conditions ranged from 52 to 65 mN/m. Statistically significant difference was observed between PAA 3.5 and PAH 7.0, representing the most and least hydrophilic films, respectively (Fig. 2B). The SFE data align well with those for the contact angle measurements, as theoretical predictions (Young's Equation) suggest that SFE increases with decreasing contact angle [44].

The thickness of PEM films (Fig. 3) is another property significantly influenced by multiple factors during the self-assembly process, especially in the case of weak polyelectrolytes. Key determinants include the polyelectrolyte's water absorption capacity, the stability of charges between polyelectrolyte pairs, and the attraction between the polyelectrolytes themselves [45]. The fabrication of multilayer thin films from weak polyelectrolytes is particularly sensitive to pH variations, leading to significant changes in thickness and enabling the regulation of both bulk and surface composition [42]. Dry thickness measurements revealed significant variations among PAA/PAH films assembled under different pH conditions (Fig. 3, white columns). In acidic pH, thicker films (58–66 nm) with higher refractive index ($n \approx 1.6$) were formed, while in neutral pH, the films tended to be thinner (10–12 nm) and had lower refractive index ($n \approx 1.4$ –1.5) (Fig. 3, white columns). These results correspond very well with the QCM-D data for film growth (Fig. 1). The increased mass and thickness can be attributed to the charge density mismatch between PAA and PAH at pH 3.5. PAA exhibits reduced ionization with more coiled conformations, while PAH is fully ionized.

At pH 7.0, both polyelectrolytes are fully charged and form flat chains with thin, more interpenetrated multilayer structures. These results aligned well with the findings of Shiratori and Rubner [42]. The slightly increased film thickness in the current study may be attributed to the higher molecular weights of the polyelectrolytes used and the inclusion of a first single layer of PEI. After dry measurements, the samples were rehydrated to simulate the physiological conditions upon the implantation of the coated biomaterials. The increase in thickness due to film rehydration depends on the assembly pH, regardless of whether the hydration was performed using water or PBS (Fig. 3). This suggests that the structural differences among the PEMs established during the assembly process remain under hydrated biological conditions.

The study revealed significant differences between dry and any hydrated state of PEMs. In contrast, variations among different hydrated conditions were less pronounced (Fig. 3). The aqueous environment (water or buffer) complexly influences film thickness, with observed statistically higher film thickness with PBS hydration (Fig. 3). The hydration levels of PEMs (Fig. 4) were assessed based on the refractive indices of the dry and hydrated PEM films after incubation in water and PBS as specified in [38]. The formula provides a simple approximation of the water content within the films: $n_{PEM} = 1.3340 \times \alpha + (1 - \alpha) \times 1.56$, where n_{PEM} is the refractive index of the hydrated PEM, 1.3340 represents the refractive index of a 0.15 M NaCl solution, 1.56 is the refractive index of a pure polymer film, and α is the fraction of water in the film [46]. By measuring the refractive index of our PEM films in both dry and hydrated states, we calculated the fraction of water (α) present in the hydrated films. The data revealed that the thin PEMs assembled at pH 7.0 exhibited higher hydration levels (47 % and 85 %, for PAH and

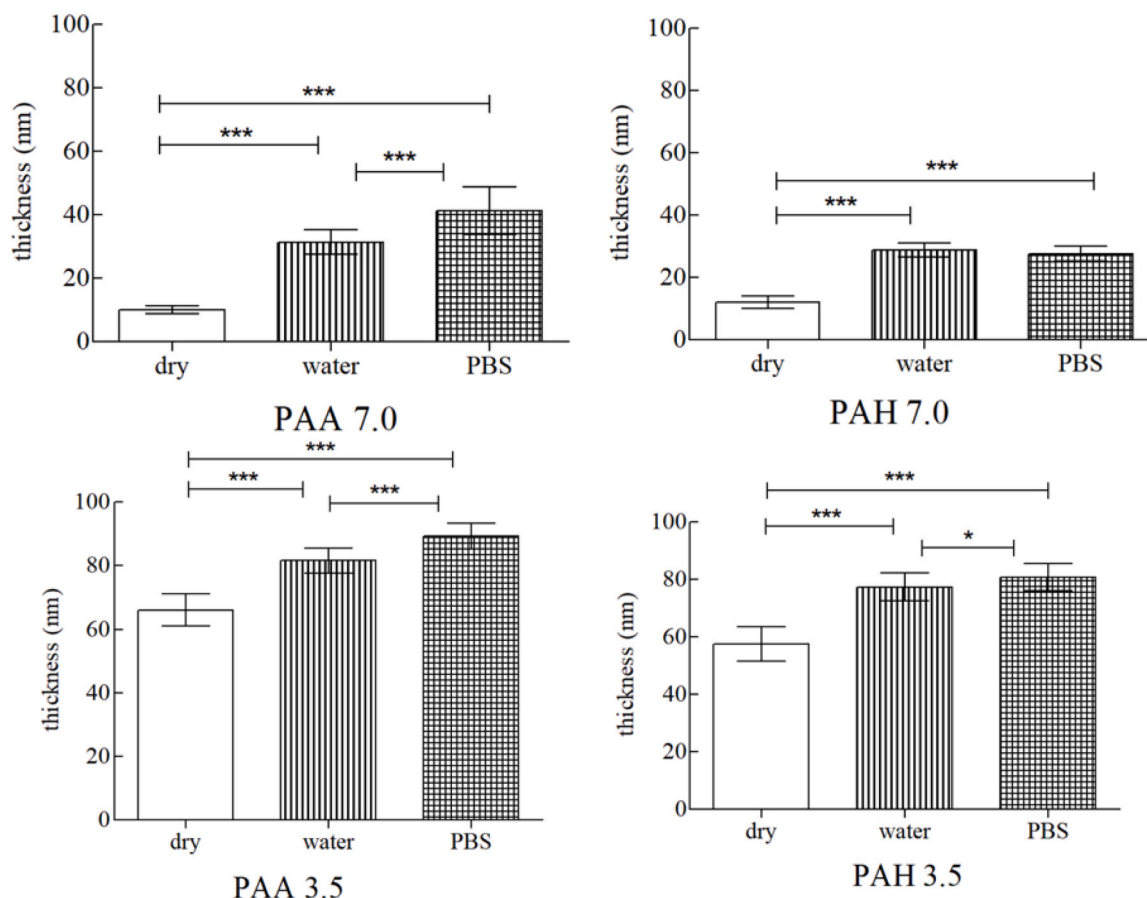


Fig. 3. Thickness variations of PEM films under different conditions: dry state, rehydrated in deionized water, and rehydrated in PBS. Data are presented as mean \pm St.Dev. Statistical significance is indicated as ns - non-significant, * - $P \leq 0.05$, *** - $P \leq 0.001$. Three independent experiments were conducted, and each sample was measured in triplicate.

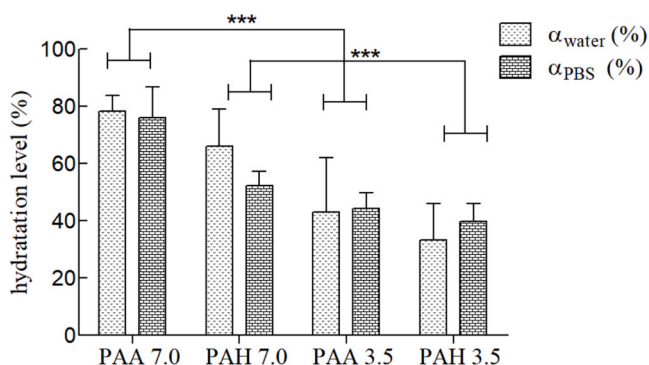


Fig. 4. Hydration levels (in %) of PAA/PAH films after their rehydration in deionized water (α_{water}) or PBS (α_{PBS}). Data are presented as mean \pm St.Dev. Statistical significance is indicated as *** - $P \leq 0.001$. Three independent experiments were conducted, and each sample was measured in triplicate.

PAA respectively) compared to those at pH 3.5 (33 % and 44 %, for PAH and PAA respectively) (Fig. 4). This finding corresponds well to the QCM-D outcome that PAA/PAH films assembled at neutral pH are more rigid than those assembled at acidic pH (Fig. 1).

Our results reveal that the pH of the assembly has a more significant impact on hydration levels than the outermost layers (PAA or PAH). The observed differences in hydration can be attributed to variations in polyelectrolyte conformation, charge density, and interlayer interactions under different assembly conditions.

The surface charge densities of four distinct PAA/PAH multilayer

films were evaluated by quantifying the adsorption of methylene blue and acid red dyes. MB, a cationic dye, was used to assess negative charges. In contrast, AR, an anionic dye, was employed to measure positive charges (Fig. 5A). This approach enabled the determination of net charge densities by summing the positive and negative charges for each sample (Fig. 5B). In the PAH 7.0 and PAH 3.5 films, the surface predominantly exhibited positive charges originating from the primary amino groups of the last deposited PAH chains. Only a minor presence of negatively charged carboxyl groups from PAA chains was detected. Consequently, the net charge of these films was positive, with PAH 7.0 being strongly positive and PAH 3.5 only weakly positive. Conversely, the PAA 7.0 and PAA 3.5 films displayed both amino and carboxyl groups on their surfaces, indicating the presence of segments from both PAA and PAH chains. Despite this, the net charges of these films were opposite in sign: negative for PAA 3.5 and unexpectedly positive for PAA 7.0. This finding aligns with previous studies indicating that at pH levels near 6.5, both PAA and PAH chains are fully charged and deposit on the surface in a fully stretched conformation, forming very thin and highly interpenetrated multilayers [22].

3.2. FNG adsorption

Studying the adsorption of FNG on polymeric surfaces is crucial for assessing their blood compatibility. FNG is considered the primary protein factor in blood coagulation, as it generates a fibrous network known as a fibrin clot during the final phase of the coagulation process [47]. FNG is cleaved upon thrombin activation, releasing fibrinopeptides and exposing the D-domains. These D-domains then interact with platelets by integrin $\alpha\text{IIb}\beta 3$ and participate in their adhesion and

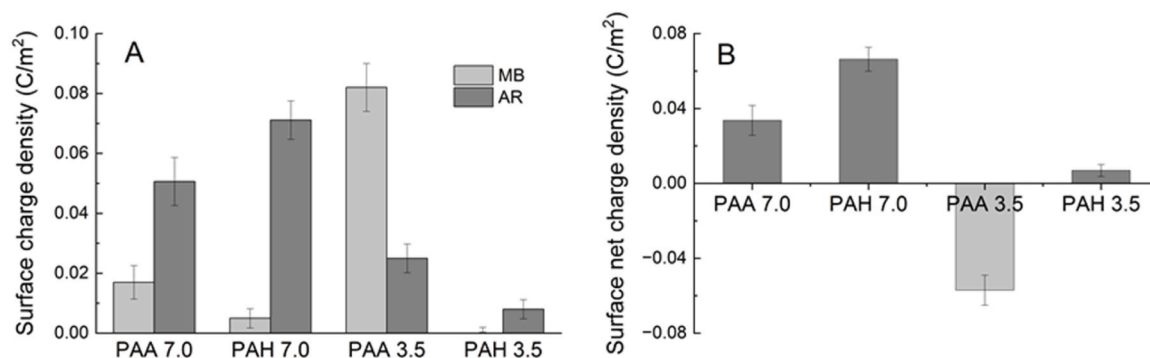


Fig. 5. (A) Surface charge density of negative charges (light gray, calculated from the absorbance of MB) and positive charges (dark grey, calculated from the absorbance of AR), and (B) surface net charges of the different PAA/PAH multilayers. Data are presented as mean \pm St.Dev. Three independent experiments were conducted, and each sample was measured in triplicate.

aggregation [9].

Consequently, QCM and EIA measurements of FNG adsorption were employed to assess the degree of FNG adsorption to PEMs and the accessibility of the D-domain in the FNG molecule upon adsorption.

3.2.1. Total amount of adsorbed FNG estimated by QCM-D

QCM-D was employed to estimate the total amount of FNG adsorbed on various PEM-coated surfaces and investigate its adsorption kinetics. The measurements revealed that the adsorption of FNG is significantly influenced by both the composition of the outermost polyelectrolyte layer and the pH during the assembly process (Fig. 6A). PAH films assembled at pH 7.0 exhibit the highest FNG adsorption (more than three times) compared to the other films. The enhanced adsorption is driven by strong electrostatic interactions between the PAH 7.0 layer and FNG molecules. FNG has an isoelectric point (pI) of approximately 5.8, rendering it negatively charged under physiological conditions (pH 7.4) [48]. This negative charge facilitates interactions with surfaces bearing positive charges such as PAH 7.0 film which exhibits a high positive surface net charge due to the protonation of amine groups in the PAH chains, confirmed through adsorption studies using dyes such as methylene blue and alizarin red (Fig. 5B). In contrast, PAA 3.5 coating possesses a negative surface charge, attributed to the deprotonation of carboxyl groups in the PAA chains. This negative charge repels the negatively charged FNG molecules, resulting in minimal adsorption onto the PAA 3.5 surfaces. The decreased adsorption of FNG on PAH 3.5 and PAA 7.0 can be explained by their weakly positive charge. These findings underscore the pivotal role of surface charge in dictating protein adsorption behaviors. In addition, the QCM-D measurements revealed a distinct manner in FNG adsorption profiles. In support of this the

analysis of frequency changes (Δf) indicated significantly higher FNG mass adsorbed on PAH 7.0 film (Fig. 6B). For instance, at the above PEM, FNG initially adsorbed rapidly, followed by a gradual equilibrium shift (Fig. 6B). In contrast, the rest of the multilayers showed slower FNG adsorption.

On the other hand, our observations indicate that FNG adsorption increases with the increase of the contact angle. This finding corroborates Vogler's assertion that protein adsorption intensifies with heightened surface hydrophobicity [49] and is in agreement with the work of Schilp S. et al., who reported that FNG adsorption initiates when the contact angle surpasses approximately 40° when using oligo (ethylene glycol)-terminated self-assembled monolayers with varying contact angles [50]. This threshold is notably lower than the commonly referred to "Berg limit" of 65° [51], suggesting that other surface characteristics can modulate the onset of protein adsorption. Our study observed that surface wettability and surface charge collectively influence FNG adsorption. Enhancing the positive surface charge reduces the contact angle threshold required for FNG adsorption, effectively lowering the "Berg limit". This phenomenon can be attributed to electrostatic interactions between the positively charged surface and the negatively charged regions of the FNG molecule, facilitating adsorption at lower than the "Berg limit" of 65° contact angles. These insights underscore the importance of considering both surface wettability and charge in the design of biomaterials' surfaces, as they jointly modulate protein adsorption behaviors.

3.2.2. FNG adsorption estimated by EIA

When FNG adsorbs onto surfaces, it may undergo conformational or orientational changes that can impact its functionality [52]. These

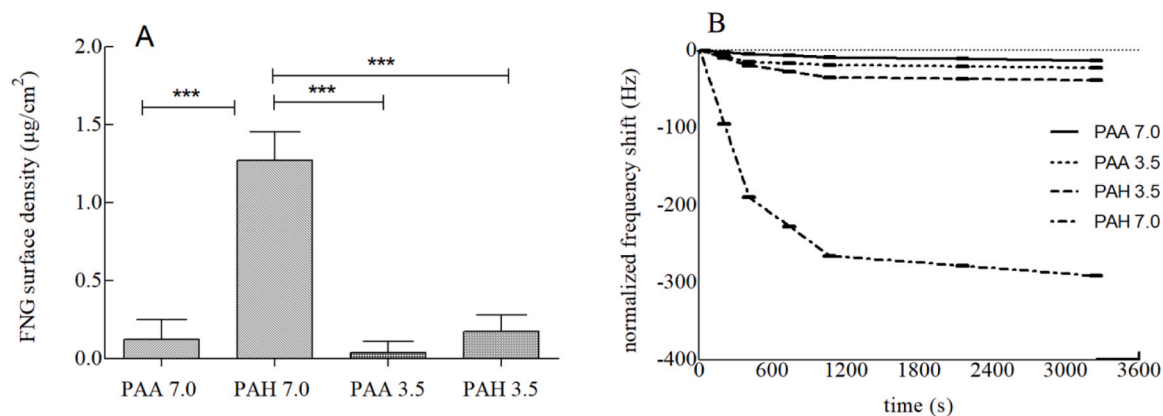


Fig. 6. (A) FNG surface density for each PEMs and (B). Normalized frequency shift relative to the initial frequency following FNG adsorption, as obtained by QCM-D. Data are presented as mean \pm St.Dev. Statistical significance is indicated as * * * - $P \leq 0.001$. Three independent experiments were conducted, and each sample was measured in triplicate.

changes could expose or hide specific domains, such as the D-domain.

We performed EIA to detect the exposition of the D-domain of FNG adsorbed on the different PAA/PAH-coated surfaces from a single FNG solution or 100 % human citrate plasma (Fig. 7). When FNG is adsorbed from a single solution, the number of accessible D-domains demonstrates a similar dependence on the assembling pH and the outermost layers as the FNG surface density measured by QCM-D (Fig. 6A and Fig. 7A). The PAH 7.0 film has the highest level of accessible D-domains (Fig. 7A). However, while the surface density of total FNG on PAH 7.0 film is about 13 times higher than those on the other surfaces (Fig. 6A), the number of accessible D-domains is only about 2 times higher (Fig. 7A). This could be due either to unfavorable protein orientation on the surface or to multilayer adsorption of FNG molecules with only the top protein layer being accessible. In general, we might suggest that this difference in protein orientation and conformation upon adsorption likely affects the accessibility of the D-domains on the surface [10]. Previous studies have also shown that FNG can undergo conformational changes of its D-domain in response to pH variations and wettability, particularly rendering the 400–411 region inaccessible on hydrophobic surfaces [14]. Other techniques, such as atomic force microscopy (AFM) or laser scanning confocal microscopy (LSCM), could be used in future cell adhesion studies to further elucidate the manner of FNG adsorption to the studied surfaces: as single molecule, in aggregates or clusters [53, 54], and its impact on cell adhesion.

Overall, the accessibility of D-domains in FNG adsorbed from human plasma is lower than when FNG is adsorbed from a single FNG solution (Fig. 7B). This trend persists across different surface treatments; notably, PAH-ended surfaces exhibit a significantly higher amount of accessible FNG D-domains compared to PAA-ended surfaces. Interestingly, pH variations do not influence this outcome, as both PAH and PAA coatings at pH 7.0 and 3.5 demonstrate comparable D-domain accessibility. The reduction observed in accessible D-domains when FNG is adsorbed from human plasma versus a single solution can be attributed to the Vroman effect [55]. This phenomenon involves the competitive adsorption of various plasma proteins, where those with higher mobility initially occupy the surface and may be partially displaced by proteins with greater surface affinity, such as FNG. Therefore, this dynamic adsorption process may induce conformational changes in the FNG molecule, potentially masking or altering the accessibility of specific domains, including the D-domains.

Among the studied physicochemical characteristics of PAA/PAH multilayers, wettability, calculated surface free energy, and surface charge, followed by film thickness and rigidity, play a role in FNG adsorption. The pH of polyelectrolyte solutions during the formation of PEMs greatly influenced the latter three physicochemical properties. For

instance, a lower pH (3.5) produced thicker, more rigid structures, while a higher pH (7.0) produced softer films. In this respect, the positively charged, the least hydrophilic, with the least surface energy, softer and thinner film PAH 7.0 film adsorbed the highest amount of FNG.

The formation and properties of polyelectrolyte multilayers constructed from weak polyelectrolytes such as PAA and PAH are highly sensitive to a variety of experimental conditions. While pH plays a critical role by modulating the degree of ionization of the polyelectrolytes and thereby influencing layer thickness, charge density, and conformation, other factors are also of great importance. These include polyelectrolyte concentration, addition of electrolytes and their concentration, the nature of the rinsing solution (e.g., deionized water vs. salt solution), and the specific deposition technique employed (such as dipping, spraying, or spin-coating). Each of these parameters can affect not only the growth regime (linear vs. exponential) but also the structural integrity, interlayer diffusion, and surface properties of the final PEM. Polyelectrolyte solution concentration is a critical parameter in PEM formation, affecting not only the thickness but also the mechanical stability, roughness, surface charge, and biological compatibility of the films. Low concentrations favor linear growth while high concentrations support exponential build-up due to diffusion of polymers into deeper layers [56,57]. Low ionic strength typically leads to thin and compact layers, with limited chain interpenetration and more linear growth. High ionic strength promotes screening of electrostatic repulsion between like-charged segments of the polyelectrolyte chains, allowing them to adopt more coiled or looped conformations. This enhances interdiffusion of chains between layers, leading to thicker films and sometimes exponential growth regimes [28,57–59]. While both dip coating and spray coating are effective for PEM fabrication, they result in distinct surface properties [60]. Dip coating offers smoother, more uniform, and predictable surfaces, ideal for detailed surface chemistry studies. Spray coating, on the other hand, is faster and scalable but may produce rougher, less uniform surfaces with different charge characteristics, factors that must be considered when tailoring interfaces for biological applications.

All of this highlights the versatility of the approach employed in this study, demonstrating that by using a single polyelectrolyte pair and modulating the process parameters during PEM self-assembly, it is possible to fine-tune protein adsorption, which is critical for optimizing the performance of biomaterials after implantation.

4. Conclusion

The study highlights the considerable correlation between the physicochemical properties of PEMs and FNG adsorption, emphasizing

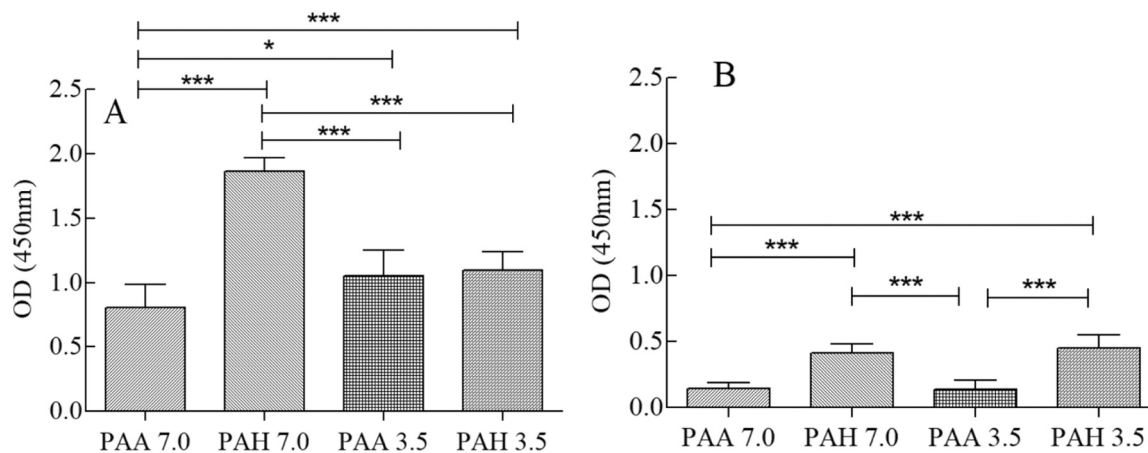


Fig. 7. (A) Detection of D-domain in FNG adsorbed from a single solution and (B) from 100 % human citrate plasma. Data are presented as mean \pm St.Dev. Statistical significance is indicated as ns - non-significant ($P > 0.05$), * - $P \leq 0.05$, ** - $P \leq 0.01$, *** - $P \leq 0.001$. Three independent experiments were conducted, and each sample was measured in triplicate.

how PEMs can influence protein-surface interactions. The study demonstrates that surface wettability, predominantly affected by the composition of the outermost layer, is essential in controlling FNG adsorption. The pH of polyelectrolyte solutions greatly affects the thickness, the rigidity of the films, and the hydration levels, resulting in thicker, more rigid structures at a lower pH (3.5) and softer films at a higher pH (7.0); however, it does not have a direct correlation with FNG adsorption levels. The results indicate that the total FNG adsorption is most significant on thinner, viscoelastic surfaces, more hydrated, less hydrophilic, and positively charged, especially on PAH-terminated PEMs at pH 7.0. At the same time, the accessibility of the D-domain (especially 400–411 region, responsible for platelet adhesion) is not expressed at such a high level on the above surfaces due to unfavorable protein orientation on the surface or to multilayer adsorption of FNG molecules. Thus, selecting appropriate PEM assembly parameters may become an attractive strategy for developing surfaces with predictable protein-surface interactions, leading to blood-contacting devices with improved biocompatibility and functionality.

CRedit authorship contribution statement

Borislava Borisova: Visualization, Investigation, Formal analysis, Data curation. **Tonya Andreeva:** Writing – original draft, Supervision, Methodology, Conceptualization. **Rumiana Tzoneva:** Writing – original draft, Supervision, Methodology, Conceptualization. **Rumen Krastev:** Supervision, Project administration, Funding acquisition. **Marina Ivanova:** Investigation, Data curation. **Irina Georgieva:** Investigation, Data curation. **Sonia Apostolova:** Investigation, Data curation.

Declaration of Competing Interest

We declare no conflict of interest. We declare that the work described has not been published previously, that it is not under consideration for publication elsewhere, that its publication is approved by all authors and tacitly or explicitly by the responsible authorities where the work was carried out, and that, if accepted, it will not be published elsewhere in the same form, in English or in any other language, including electronically without the written consent of the copyright-holder.

Acknowledgments

B.B. acknowledges funding from the German Academic Exchange Service (DAAD) through the Forschungsstipendien - Bi-national betreute Promotionen/Cotutelle program (2023/24, No. 57645446) for the research stay at Reutlingen University, Germany. B.B., R.T., and S.A. acknowledge financial support from the PhD program of the Ministry of Education and Science of Bulgaria. T.A. and R.K. gratefully acknowledge the funding by the German Research Foundation (Deutsche Forschungsgemeinschaft, DFG), Research Unit FOR5250 “Permanent and bioresorbable implants with tailored functionality” (No. 449916462). Dr. Frank K. Göring (qCell T, 3 t Analytik, Tuttlingen, Germany) is acknowledged for providing the QCM device used in this study.

Data availability

Data will be made available on request.

References

- J.B. Schlenoff, Charge balance and transport in ion-paired polyelectrolyte multilayers. *Multilayer Thin Films: Sequential Assembly of Nanocomposite Materials*, Wiley-VCH Verlag GmbH & Co. KGaA, Weinheim, Germany, 2012, pp. 281–320.
- H. Hartmann, R. Krastev, Biofunctionalization of surfaces using polyelectrolyte multilayers, *BioNanoMaterials* 18 (1-2) (2017) 20160015, <https://doi.org/10.1515/bnm-2016-0015>.
- J. Enderle, J. Bronzino. *Introduction to Biomedical Engineering*, 3rd, Elsevier Academic press, Amsterdam, 2012.
- R. Vilar, R.J. Fish, A. Casini, M. Neerman-Arbez, Fibrin (ogen) in human disease: both friend and foe, *Haematologica* 105 (2) (2020) 284–296, <https://doi.org/10.3324/haematol.2019.236901>.
- A. Frutiger, A. Tanno, S. Hwu, R.F. Tiefenauer, J. Voros, N. Nakatsuka, Nonspecific binding-fundamental concepts and consequences for biosensing applications, *Chem. Rev.* 121 (13) (2021) 8095–8160, <https://doi.org/10.1021/acs.chemrev.1c00044>.
- S. Rodrigues, I. Gonçalves, M. Martins, M. Barbosa, B. Ratner, Fibrinogen adsorption, platelet adhesion and activation on mixed hydroxyl-/methyl-terminated self-assembled monolayers, *Biomater* 27 (31) (2006) 5357–5367, <https://doi.org/10.1016/j.biomaterials.2006.06.010>.
- T.H. Groth, K. Klosz, E.J. Campbell, R.R.C. New, B. Hall, H. Goering, Protein adsorption, lymphocyte adhesion and platelet adhesion/activation on polyurethane ureas is related to hard segment content and composition, *J. Biomater. Sci. Polym. Ed.* 6 (6) (1995) 497–510, <https://doi.org/10.1163/156856294x00464>.
- D. Kiaei, A.S. Hoffman, T.A. Horbett, K.R. Lew, Platelet and monoclonal antibody binding to fibrinogen adsorbed on glow-discharge-deposited polymers, *J. Biomed. Mater. Res.* 29 (6) (1995) 729–739, <https://doi.org/10.1002/jbm.820290609>.
- R. Tzoneva, M. Heuchel, T. Groth, G. Altankov, W. Albrecht, D. Paul, Fibrinogen adsorption and platelet interactions on polymer membranes, *Biomater. Sci. Polym. Ed.* 13 (9) (2002) 1033–1050, <https://doi.org/10.1163/156856202760319171>.
- T.A. Horbett, Fibrinogen adsorption to biomaterials, *J. Biomed. Mater. Res.* A 106 (10) (2018) 2777–2788, <https://doi.org/10.1002/jbm.a.36460>.
- P.K. Patibandla, N. Tyagi, W.L. Dean, S.C. Tyagi, A.M. Roberts, D. Lominadze, Fibrinogen induces alterations of endothelial cell tight junction proteins, *J. Cell Physiol.* 221 (1) (2009) 195–203, <https://doi.org/10.1002/jcp.21845>.
- Z. Zhang, B. Casey, D.K. Galanakis, C. Marmorat, S. Skoog, K. Vorvolakos, M. Simon, M.H. Rafailovich, The influence of surface chemistry on adsorbed fibrinogen conformation, orientation, fiber formation and platelet adhesion, *Acta Biomater.* 54 (2017) 164–174, <https://doi.org/10.1016/j.actbio.2017.03.002>.
- P. Roach, D. Farrar, C.C. Perry, Interpretation of protein adsorption: surface-induced conformational changes, *JACS* 127 (22) (2005) 8168–8173, <https://doi.org/10.1021/ja042898o>.
- A.E. Nel, L. Mädler, D. Velegol, T. Xia, E.M. Hoek, P. Somasundaran, F. Klaessig, V. Castranova, M. Thompson, Understanding biophysicochemical interactions at the nano-bio interface, *Nat. Mater.* 8 (7) (2009) 543–557, <https://doi.org/10.1038/nmat2442>.
- M. Rabe, D. Verdes, S. Seeger, Understanding protein adsorption phenomena at solid surfaces, *Adv. Colloid Interface Sci.* 162 (1-2) (2011) 87–106, <https://doi.org/10.1016/j.cis.2010.12.007>.
- T.C. Ta, M.T. McDermott, Mapping interfacial chemistry induced variations in protein adsorption with scanning force microscopy, *Anal. Chem.* 72 (11) (2000) 2627–2634, <https://doi.org/10.1021/ac991137e>.
- G. Khot, F. Kuforiji, R. Wright, P. Roach, Dynamic assessment of fibrinogen adsorption and secondary structure perturbation, in: *Conference Papers in Science*. Hindawi Publishing Corporation. 2014(1) 601546. <https://doi.org/10.1155/2014/601546.2014>.
- I. Lynch, K.A. Dawson, S. Linse, Detecting cryptic epitopes created by nanoparticles, *Sci. s. STKE* 2006 (327) (2006) pe14, <https://doi.org/10.1126/stke.3272006pe14>, pe14.
- M. Assfalg, Protein adsorption and conformational changes, *Molecules* 26 (23) (2021) 7079, <https://doi.org/10.3390/molecules26237079>.
- M.J. Penna, M. Mijajlovic, M.J. Biggs, Molecular-level understanding of protein adsorption at the interface between water and a strongly interacting uncharged solid surface, *JACS* 136 (14) (2014) 5323–5331, <https://doi.org/10.1021/ja411796e>.
- C.F. Wertz, M.M. Santore, Fibrinogen adsorption on hydrophilic and hydrophobic surfaces: geometrical and energetic aspects of interfacial relaxations, *Langmuir* 18 (3) (2002) 706–715, <https://doi.org/10.1021/la011075z>.
- X. Wu, C. Wang, P. Hao, F. He, Z. Yao, X. Zhang, Adsorption properties of albumin and fibrinogen on hydrophilic/hydrophobic TiO₂ surfaces: a molecular dynamics study, *Coll. Surf. B Biointerfaces* 207 (2021) 111994, <https://doi.org/10.1016/j.colsurfb.2021.111994>.
- T. Andreeva, A. Rudt, L. Fábíán, F. Ayaydin, I. Iliev, O. Jung, M. Barbeck, A. Dér, R. Krastev, S.G. Taneva, Control of cell adhesion and growth on polysaccharide-based multilayer coatings by incorporation of graphene oxide, *Coatings* 14 (5) (2024) 570, <https://doi.org/10.3390/coatings14050570>.
- M. Kolasirińska, R. Krastev, P. Warszyński, Characteristics of polyelectrolyte multilayers: effect of PEI anchoring layer and posttreatment after deposition, *J. Colloid Interface Sci.* 305 (1) (2007) 46–56, <https://doi.org/10.1016/j.jcis.2006.09.035>.
- V. Izumrudov, S.A. Sukhishvili, Ionization-controlled stability of polyelectrolyte multilayers in salt solutions, *Langmuir* 19 (13) (2003) 5188–5191, <https://doi.org/10.1021/la034360m>.
- C. Brunot, L. Ponsonnet, C. Lagneau, P. Farge, C. Picart, B. Grosgeat, Cytotoxicity of polyethyleneimine (PEI), precursor base layer of polyelectrolyte multilayer films, *Biomaterials* 28 (4) (2007) 632–640, <https://doi.org/10.1016/j.biomaterials.2006.09.026>.
- P. Tryoen-Tóth, D. Vautier, Y. Haikel, J.C. Voegel, P. Schaaf, J. Chluba, J. Ogier, Viability, adhesion, and bone phenotype of osteoblast-like cells on polyelectrolyte multilayer films, *J. Biomed. Mater. Res.* 60 (4) (2002) 657–667, <https://doi.org/10.1002/jbm.10110>.
- G. Decher, Fuzzy nanoassemblies: toward layered polymeric multicomposites, *Science* 277 (5330) (1997) 1232–1237, <https://doi.org/10.1126/science.277.5330.1232>.

- [29] P.T. Hammond, Form and function in multilayer assembly: new applications at the nanoscale, *Adv. Mater.* 16 (15) (2004) 1271–1293, <https://doi.org/10.1002/adma.200400760>.
- [30] C.J. Detzel, A.L. Larkin, P. Rajagopalan, Polyelectrolyte multilayers in tissue engineering, *Tissue Eng. Part B Rev.* 17 (2) (2011) 101–113, <https://doi.org/10.1089/ten.teb.2010.0548>.
- [31] T.D. Andreeva, O. Walker, A. Rudt, O. Jung, M. Barbeck, M. Gülcher, R. Krastev, Composite polymer/wax coatings as a corrosion barrier of bioresorbable magnesium coronary stents, *Heliyon* 10 (13) (2024) e34025, <https://doi.org/10.1016/j.heliyon.2024.e34025>.
- [32] J.B. Schlenoff, S.T. Dubas, Mechanism of polyelectrolyte multilayer growth: charge overcompensation and distribution, *Macromolecules* 34 (3) (2001) 592–598, <https://doi.org/10.1021/ma0003093>.
- [33] C.C. Buron, C. Filiatre, F. Membrey, C. Bainier, D. Charrat, A. Foissy, Early steps in layer-by-layer construction of polyelectrolyte films: the transition from surface/polymer to polymer/polymer determining interactions, *J. Coll. Int. Sci.* 314 (2) (2007) 358–366, <https://doi.org/10.1016/j.jcis.2007.05.060>.
- [34] R. Bryaskova, N. Georgieva, T. Andreeva, R. Tzoneva, Cell adhesive behavior of PVA-based hybrid materials with silver nanoparticles, *Surf. Coat. Tech.* 235 (2013) 186–191, <https://doi.org/10.1016/j.surfcoat.2013.07.032>.
- [35] D.K. Owens, R.C. Wendt, Estimation of the surface free energy of polymers, *J. Appl. Polym. Sci.* 13 (8) (1969) 1741–1747, <https://doi.org/10.1002/app.1969.070130815>.
- [36] S. Ilyas, N. Joseph, A. Szymczyk, A. Volodin, K. Nijmeijer, W.M. De Vos, I. F. Vankelecom, Weak polyelectrolyte multilayers as tunable membranes for solvent-resistant nanofiltration, *J. Membr. Sci.* 514 (2015) 322–331, <https://doi.org/10.1016/j.memsci.2016.04.073>.
- [37] G. Sauerbrey, Verwendung von Schwingquarzen zur Wägung dünner Schichten und zur Mikrowägung, *Z. Phys.* 155 (1959) 206–222, <https://doi.org/10.1007/BF01337937>.
- [38] G. Liu, G. Zhang, G. Liu, G. Zhang, Basic principles of QCM-D, in: *QCM-D Studies on Polymer Behavior at Interfaces*, Springer, 2013, pp. 1–8, [10.1007/978-3-642-39790-5_1](https://doi.org/10.1007/978-3-642-39790-5_1).
- [39] K.K. Kanazawa, J.G. Gordon, The oscillation frequency of a quartz resonator in contact with liquid, *Anal. Chim. Acta* 175 (1985) 99–105, [https://doi.org/10.1016/S0003-2670\(00\)82721-X](https://doi.org/10.1016/S0003-2670(00)82721-X).
- [40] F.K. Gehring. *Schwingungssensorik in Flüssigkeiten*, Cuvillier Verlag Göttingen, 2006.
- [41] P. Bieker, M. Schönhoff, Linear and exponential growth regimes of multilayers of weak polyelectrolytes in dependence on pH, *Macromolecules* 43 (11) (2010) 5052–5059, <https://doi.org/10.1021/ma1007489>.
- [42] M.F. Rubner, S.S. Shiratori, pH-dependent thickness behavior of sequentially adsorbed layers of weak polyelectrolytes, *Macromolecules* 33 (2000) 4213–4219, <https://doi.org/10.1021/ma991645q>.
- [43] M. Todica, C.V. Pop, L. Udrescu, T. Stefan, Spectroscopy of a gamma irradiated poly (Acrylic Acid)-Clotrimazole system, *Chin. Phys. Lett.* 28 (12) (2011) 128201, <https://doi.org/10.1088/0256-307X/28/12/128201>.
- [44] T. Young, An essay on the cohesion of fluids, *Philos. Trans. R. Soc. Lond.* 95 (1805) 65–87, <https://doi.org/10.1098/rstl.1805.0005>.
- [45] R. V. Klitzing, Internal structure of polyelectrolyte multilayer assemblies, *Phys. Chem. Chem. Phys.* 8 (43) (2006) 5012–5033, <https://doi.org/10.1039/B607760A>.
- [46] C. Picart, Polyelectrolyte multilayer films: from physico-chemical properties to the control of cellular processes, *Curr. Med. Chem.* 15 (7) (2008) 685–697, <https://doi.org/10.2174/092986708783885219>.
- [47] S. Köhler, F. Schmid, G. Settanni, The internal dynamics of fibrinogen and its implications for coagulation and adsorption, *PLoS Comp. Biol.* 11 (9) (2015) e1004346, <https://doi.org/10.1371/journal.pcbi.1004346>.
- [48] M. Wasilewska, Z. Adamczyk, B. Jachimska, Structure of fibrinogen in electrolyte solutions derived from dynamic light scattering (DLS) and viscosity measurements, *Langmuir* 25 (6) (2009) 3698–3704, <https://doi.org/10.1021/la803662a>.
- [49] E.A. Vogler, Structure and reactivity of water at biomaterial surfaces, *Adv. Colloid Interface Sci.* 74 (1-3) (1998) 69–117, [https://doi.org/10.1016/S0001-8686\(97\)00040-7](https://doi.org/10.1016/S0001-8686(97)00040-7).
- [50] S. Schilp, A. Kueller, A. Rosenhahn, M. Grunze, M.E. Pettitt, M.E. Callow, J. A. Callow, Settlement and adhesion of algal cells to hexa (ethylene glycol)-containing self-assembled monolayers with systematically changed wetting properties, *Biointerphases* 2 (4) (2007) 143–150, <https://doi.org/10.1116/1.2806729>.
- [51] E.A. Vogler, J.C. Graper, H.W. Sugg, L.M. Lander, W.J. Brittain, Contact activation of the plasma coagulation cascade. II. Protein adsorption to procoagulant surfaces, *J. Biomed. Mater. Res.* 29 (1995) 1017–1028, <https://doi.org/10.1002/jbm.820290814>.
- [52] M.L. Clarke, J. Wang, Z. Chen, Conformational changes of fibrinogen after adsorption, *J. Phys. Chem. B* 109 (46) (2005) 22027–22035, <https://doi.org/10.1021/jp054456k>.
- [53] K.L. Marchin, S. Phung, C.L. Berrie, Evidence for fibrinogen mobility on hydrophobic surfaces, *e-JSSNT* 3 (2005) 173–178, <https://doi.org/10.1380/ejsnt.2005.173>.
- [54] L. Zhang, B. Casey, D.K. Galanakis, C. Marmorat, S. Skoog, K. Vorvolakos, M. Simon, M.H. Rafailovich, The influence of surface chemistry on adsorbed fibrinogen conformation, orientation, fiber formation and platelet adhesion, *Acta Biomater.* 54 (2017) 164–174, <https://doi.org/10.1016/j.actbio.2017.03.002>.
- [55] S.L. Hirsh, D.R. McKenzie, N.J. Nosworthy, J.A. Denman, O.U. Sezerman, M. M. Bilek, The Vroman effect: competitive protein exchange with dynamic multilayer protein aggregates, *Colloids Surf. B Biointerfaces* 103 (2013) 395–404, <https://doi.org/10.1016/j.colsurfb.2012.10.039>.
- [56] C. Porcel, P. Lavalle, G. Decher, B. Senger, J.C. Voegel, P. Schaaf, Influence of the polyelectrolyte molecular weight on exponentially growing multilayer films in the linear regime, *Langmuir* 23 (4) (2007) 1898–1904, <https://doi.org/10.1021/la062728k>.
- [57] T. Andreeva, T. Drieschner, D.S. Golovko, A. Lorenz, K. Rebner, R. Krastev, Process validation and a new method for quality control of ultrathin polyelectrolyte multilayer coatings, *Coll. Surf. A Physicochem. Eng. Asp.* 676 (2023) 132157, <https://doi.org/10.1016/j.colsurfa.2023.132157>.
- [58] A.A. Antipov, G.B. Sukhorukov, H. Möhwald, Influence of the ionic strength on the polyelectrolyte multilayers' permeability, *Langmuir* 19 (6) (2003) 2444–2448, <https://doi.org/10.1021/la026101n>.
- [59] K. Tang, N.A. Besseling, Formation of polyelectrolyte multilayers: ionic strengths and growth regimes, *Soft Matter* 12 (4) (2016) 1032–1040, <https://doi.org/10.1039/C5SM02118A>.
- [60] M. Kolasinska, R. Krastev, T. Gutberlet, P. Warszynski, Layer-by-layer deposition of polyelectrolytes. Dipping versus spraying, *Langmuir* 25 (2) (2009) 1224–1232, <https://doi.org/10.1021/la803428f>.